Altered neocortical tactile but preserved auditory early change detection responses in Friedreich ataxia.

Running title: sensory change detection in Friedreich ataxia

Gilles Naeije[1,2], Vincent Wens[2,3], Mathieu Bourguignon[2,4,5], Serge Goldman[2,3], Massimo Pandolfo[1,6] and Xavier De Tiège[2,3].

[1]Service of Neurology, CUB Hôpital Erasme, Université libre de Bruxelles (ULB), Brussels, Belgium.

[2]Laboratoire de Cartographie fonctionnelle du Cerveau (LCFC), UNI – ULB Neuroscience Institute, Université libre de Bruxelles (ULB), Brussels, Belgium.

[3]Magnetoencephalography Unit, Department of Functional Neuroimaging, Service of Nuclear Medicine, CUB Hôpital Erasme, Université libre de Bruxelles (ULB), Brussels, Belgium.

[4]Laboratoire Cognition Langage et Développement, UNI – ULB Neuroscience Institute, Université libre de Bruxelles (ULB), Brussels, Belgium.

[5]BCBL, Basque Center on Cognition, Brain and Language, 20009 San Sebastian, Spain.

[6] Laboratoire de Neurologie Expérimentale, UNI – ULB Neuroscience Institute, Université libre de Bruxelles (ULB), Brussels, Belgium.

Corresponding author:

Gilles Naeije, Laboratoire de Cartographie fonctionnelle du Cerveau (LCFC), ULB Neuroscience Institute, 808, route de Lennik, 1070 Brussels, Belgium.
Tel: +3225558196 Fax: +3225553942 e-mail: gilles.naeije@erasme.ulb.ac.be

Highlights

- MEG has a higher sensitivity to SI cortex responses than evoked potentials in FRDA
- Neuromagnetic responses at SI cortex are delayed and reduced in amplitude in FRDA
- Tactile MMN responses at SII cortex are reduced and delayed in FRDA

Abstract

Objective: To study using magnetoencephalography (MEG) the spatio-temporal dynamics of neocortical responses involved in sensory processing and early change detection in Friedreich ataxia (FRDA).

Methods: Tactile (TERs) and auditory (AERs) evoked responses, and early neocortical change detection responses indexed by the mismatch negativity (MMN) were recorded using tactile and auditory oddballs in sixteen FRDA patients and matched healthy subjects. Correlations between the maximal amplitude of each response, genotype and clinical parameters were investigated.

Results: Evoked responses were detectable in all FRDA patients but one. In patients, TERs were delayed and reduced in amplitude, while AERs were only delayed. Only tactile MMN responses at the contralateral secondary somatosensory cortex were altered in FRDA patients. Maximal amplitudes of TERs, AERs and tactile MMN correlated with genotype, but did not correlate with clinical parameters.

Conclusions: In FRDA, the amplitude of tactile MMN responses at SII cortex are reduced and correlate with the genotype, while auditory MMN responses are not altered.

Significance: Somatosensory pathways and tactile early change detection are selectively impaired in FRDA.

Keywords: mismatch negativity, secondary somatosensory cortex, cerebellum, Friedreich ataxia, magnetoencephalography.

Abbreviations:

AERs: neocortical auditory evoked responses
AI: primary auditory cortex
amMMN: auditory magnetic MMN
aMMN: auditory MMN
cAI: contralateral primary auditory cortex
cSI: contralateral primary auditory cortex
cSII: contralateral secondary somatosensory cortex
cEMFs : cortical evoked magnetic fields
D: Deviants
dSPM: dynamic statistical parametric mapping
ECG: electrocardiogam
EFACTS: European Friedreich's Ataxia Consortium for Translational Studies
EOGs: electrooculograms
FRDA: Friedreich ataxia
FXN: frataxin
ICA: independent component analysis
MEG: magnetoencephalography
MLR: middle latency responses
MMN: Mismatch negativity
MNI: Montreal institute of Neurology
MSR: magnetic shielded room
OP1: first cytoarchitectonic subdivision of the parietal operculum
S: Standards
SARA: Scale for the Assessment and Rating of Ataxia
SI: primary somatosensory cortex
SII: secondary somatosensory cortex
smMMN: somatosensory magnetic MMN
sMMN: somatosensory MMN
SSEPs: cortical somatosensory evoked potentials
tDCS: transcranial direct current stimulation
TERs: neocortical tactile evoked responses

Introduction

Friedreich ataxia (FRDA) is the most common form of recessive inherited ataxia in Caucasians (Ruano et al. 2014) with a prevalence of 3-4/100000 (Schulz et al. 2009). It is caused in most patients by homozygosity for a GAA1 trinucleotide repeat expansion in the first intron of the frataxin (FXN) gene (Campuzano et al. 1996), encoding the mitochondrial protein FXN. Expanded GAA1 repeats lead to FXN deficiency causing mitochondrial dysfunction and, ultimately, cell death (González-Cabo and Palau 2013). In humans, FXN mRNA is most abundant in tissues affected by FRDA (Pandolfo 2008), partly explaining their selective vulnerability. FRDA was initially described in 1863 by Nikolaus Friedreich as a spinal disorder characterized by an atrophy of the spinal posterior columns (Friedreich 1863). Loss of large primary sensory neurons in the dorsal root ganglia (DRGs), and consequently of large myelinated fibers in sensory nerves and in the posterior columns of the spinal cord is the pathological hallmark of FRDA. It is an early phenomenon, considered by some to be developmental more than degenerative (Mascalchi et al. 2017), though signs of active neuronal loss and inflammation persist in DRGs throughout life (Koeppen et al. 2016). Atrophy of Clarke column and loss of spinocerebellar fibers follow the loss of primary proprioceptive neurons in DRGs (Koeppen and Mazurkiewicz 2013). The cerebellum also develops intrinsic pathology affecting the dentate nucleus and consequently its efferent fibers in the superior cerebellar peduncle (Koeppen and Mazurkiewicz 2013), while cortical cerebellar atrophy is at most discrete (Koeppen and Mazurkiewicz 2013; Selvadurai et al. 2016). Compared to DRG and spinal pathology, cerebellar involvement in FRDA is of later onset, after symptoms have appeared, being clearly degenerative in nature. Clinically, these structural lesions lead to a “tabetocerebellar gait” ataxic pattern combining afferent proprioceptive and cerebellar ataxia (for a review, see, e.g., Pandolfo, 2008).

The early, scarcely progressive, possibly developmental character of DRG pathology is supported by neurophysiological studies that show amplitude reduction of cortical somatosensory evoked potentials (SSEPs) correlating with the size of GAA1 triplet expansion and not with disease duration (Ouvrier et al. 1982; Said et al. 1986; Santoro et al. 1999). Still, part of the somatosensory impairments in FRDA could also be accounted by the progressive cerebellar degeneration. Indeed, in healthy subjects, the posterior lobe of the cerebellum and the ventral parts of the dentate nuclei contribute to sensory and perceptual processes (for reviews, see, e.g., Baumann et al., 2015; Leggio & Molinari, 2015), particularly in the selection of pertinent stimuli, attentional orientation and focusing. These processes require detecting changes in the temporal regularity (Moberget et al. 2008; Kotz et al. 2014) and in the physical features (Clark et al. 2000)of sensory stimuli.

The mismatch negativity (MMN) is the electromagnetic signal that reflects the early cortical response to a change in a sensory stimulus. It is elicited by rare stimuli (i.e., deviants) inserted into a sequence of repeated stimuli (i.e., standards) (for reviews, see, e.g.,Garrido, Kilner, Stephan, & Friston, 2009). MMN has been described for the auditory (aMMN) (Naatanen and Alho 1995) somatosensory (sMMN) (Kekoni et al. 1997) and visual (Czigler I, Balázs L 2002) modalities. Interestingly, two studies performed in patients with cerebellar disorders showed prominent sMMN alteration ipsilaterally to cerebellar hemispheric lesions, but normal pitch aMMN (Restuccia et al. 2007; Moberget et al. 2008). Furthermore, cerebellar transcranial direct current stimulation (tDCS) in healthy subjects modulates sMMN but not aMMN. These findings suggest a role of the cerebellum in somatosensory change detection compared to the auditory modality. Previous functional neuroimaging studies identified the secondary somatosensory (SII) cortex as the main sMMN generator (Downar et al. 2000; Akatsuka et al. 2005; Naeije et al. 2016, 2017). Thus, the functional role of the

cerebellum in somatosensory change detection might be exerted by affecting SII cortex activity.

To test this hypothesis, we compared somatosensory and auditory MMN responses in FRDA patients, where primary sensory and cerebellar pathology coexist. Besides investigating how these pathologies evolve and interact in FRDA, this study aimed at getting further insights into the neural network involved in sensory change detection, and in particular how the cerebellum differentially affects sMMN and aMMN. For that purpose, we used magnetoencephalography (MEG) to investigate in a large population of FRDA patients the cortical evoked magnetic fields (cEMFs) elicited by tactile and auditory change detection by comparison with matched healthy subjects. A prerequisite to the interpretation of MMN responses in FRDA patients was the characterization of cEMFs elicited by tactile and auditory stimuli at primary sensory cortices. Contrary to EEG used to detect SSEPs, MEG provides heightened sensitivity and signal-to-noise ratio for neocortical sources on the sides of sulci, such as the hand representations at primary somatosensory (SI) and SII cortices (Goldenholz et al. 2009; Hunold et al. 2016; Puce and Hamalainen 2017). Accordingly, by using MEG, we expected to detect cortical responses to tactile hand stimuli in a larger proportion of FRDA patients than in previous studies that used SSEPs, in which responses could only be recorded in 1/3 to 2/3 of FRDA patients (Jones et al. 1980; Pelosi et al. 1984; Vanasse et al. 1988; Santoro et al. 1999, 2000; Santiago-Perez et al. 2007). We also tested the specific hypothesis that the magnetic sMMN (smMMN) at SII cortex contralateral to the tactile stimulation would be altered in FRDA patients possibly due to the FRDA-related cerebellar involvement while the magnetic aMMN (amMMN) would not. We also assessed to what extent smMMN responses would correlate in FRDA patients with disease duration, GAA1 triplet expansion and patients' clinical parameters.

Materials and Methods

Participants

Sixteen right-handed adults with genetically proven FRDA (10 females, six males, age 27.8 ± 12.6 years) were included in this study. Of notice, one patient was heterozygous for a GAA1 repeat expansion and had a point mutation in the *FXN* gene. All patients were included in the European Friedreich's Ataxia Consortium for Translational Studies (EFACTS, http://www.e-facts.eu/html/studies/project/concept) clinical study, which collects demographic, genetic, and prospective clinical data such as SARA scores. Handedness was defined, as in EFACTS, according to the patients' report of their preferred hand for the use of objects in daily life tasks. Table 1 summarizes the patients' clinical characteristics.

Nine patients (five females, age 35.8 ± 10.9 years, mean GAA1 621 ± 225, mean SARA 24 ±7.5) also accepted to undergo SSEPs recording using electrical stimulation of the right median nerve. Recording and analysis of SSEPs were done as in Santoro et al. (2000) except that, for comfort reasons, the two trials consisted of 256 epochs rather than 1000 epochs.

As controls, we recruited 16 healthy right-handed adult subjects without any history of neurological or psychiatric disorder, who were matched to FRDA patients for age and sex (10 females, six males, age 28 ± 13 years).

All participants provided written informed consent. The study was approved by the CUB-Hôpital Erasme Ethics Committee (Reference EudraCT/CCB: B406201317212).

Experimental Paradigm

Participants underwent three experimental conditions: a unilateral somatosensory oddball paradigm, a monaural auditory oddball paradigm, and a five minutes resting-state period. They were instructed to gaze at a cross on the wall of the magnetically shielded room

(MSR) during each condition. The order of the three conditions was randomized across participants. In those oddballs, participants were exposed to 600 stimuli in each modality of which 500 were standards and 100 deviants.

Figure 1 illustrates the oddball paradigms used to elicit the somatosensory and auditory brain responses.

In the tactile oddball paradigm, derived from (Naeije et al. 2016, 2017), stimuli were applied using a pneumatic stimulator, as described in (Wienbruch et al. 2006). Standards were applied to the right index fingertip (stimulated area: 1 cm^2, intensity: 2 bars, duration: 50 ms), while deviants consisted in the simultaneous stimulation of the fingertip and the middle phalanx of the right index finger. Importantly, all FRDA patients felt the difference between standards and deviants during a preliminary test stimulation done outside the MSR. Pneumatic tactile stimuli were preferred to peripheral nerve electrical stimulation not only because they are more natural and not unpleasant, but also because electrical stimuli activate simultaneously a large number of fibers with different conduction velocities, bypassing peripheral mechanoreceptors as well as the distal part of peripheral nerves (Naeije et al. 2017). Standards and deviants were applied on the same finger in order to recruit as much as possible common peripheral and cortical pathways (Naeije et al. 2017). Of note, the fact that more skin mechanoreceptors are stimulated by deviants than by standards is not of concern, as we previously showed that smMMN responses do not change if such standards and deviants are flipped (Naeije *et al*., 2016).

For the auditory oddball paradigm, derived from (Bekinschtein et al. 2009), stimuli consisted in audible tones (50 ms duration, 10 ms rise, 10 ms fall) of 540 Hz (standards) or 600 Hz (deviants) that were presented in participants' right hear using an Etymotic ER-3A (Etymotic Research Inc., Illinois, USA) earphone at a comfortable volume. Participants wore

Etymotic ER-3A earphones in both ears during the entire experiment to suppress auditory noise, particularly generated by the pneumatic stimulation.

For each oddball paradigm, blocks of five stimuli were applied with an inter-stimulus interval (ISI) of 500 ms. Each block comprised either four standards followed by a deviant (SSSSD, standard block) or five standards (SSSSS, deviant block). Each deviant within standard SSSSD blocks broke a sequence of four identical stimuli, hence leading to a local change expected to generate a MMN response (Bekinschtein et al. 2009; Wacongne et al. 2011; Chennu et al. 2013; Naeije et al. 2016). One hundred and twenty blocks were administered in each oddball condition to participants with an inter-block interval (IBI) of 800 ms. The first 20 blocks were always standard (SSSSD) blocks, whereas the subsequent 100 blocks consisted of 20 deviant (SSSSS) blocks randomly intermingled among 80 standard (SSSSD) blocks, with the only constraint that two deviant blocks could not occur successively. Deviant (SSSSS) blocks were used to lower the predictability of deviant stimuli occurrence within standard (SSSSD) blocks as the cerebellum is thought to be involved in sensory change detection through predictions about upcoming sensory events. Furthermore, in this paradigm participants were asked to count the number of deviant (SSSSS) blocks, thereby limiting attentional fluctuations along the oddball paradigms.

The resting-state recording lasted five minutes, during which participants were instructed to relax, not to move and to gaze at a fixation point in the MSR to avoid any eye movements.

Data Acquisition

Participants' neuromagnetic activity was recorded using a whole-scalp-covering MEG device (Neuromag Vectorview, Elekta Oy, 12 FRDA patients, seven controls; Triux, MEGIN, four FRDA patients, nine controls; Helsinki, Finland), installed in a lightweight MSR (Maxshield, MEGIN, Helsinki, Finland)(De Tiège et al. 2008). The MEG sensor layout

consisted in 102 sensor triplets, each comprising one magnetometer and two orthogonal planar gradiometers characterized by different patterns of spatial sensitivity to right beneath or nearby cortical sources. Four head-tracking coils monitored participants' head position inside the MEG helmet. The location of the coils and at least 150 head-surface (on scalp, nose and face) points with respect to anatomical fiducials were determined with an electromagnetic tracker (Fastrak, Polhemus, Colchester, VT, USA). Eye movements and blinks were monitored with vertical and horizontal electrooculograms (EOGs). An electrocardiogam (ECG) was also recorded using bipolar electrodes placed below the clavicles. All signals were sampled at 1 kHz with online band-pass filter at 0.1–330 Hz. Subjects' high-resolution 3D-T1 cerebral magnetic resonance images (MRIs) were acquired on a 1.5 T MRI scanner (Intera, Philips, Netherlands).

MEG data preprocessing

Continuous MEG data were first preprocessed off-line with the signal space separation (SSS) method to subtract external interferences and correct for head movements (Taulu et al. 2005). Then, ocular and cardiac artifacts were suppressed using an independent component analysis (ICA). Specifically, the filtered data (off-line band-pass: 0.1-45 Hz) were divided into 1-s-long epochs. Epochs with large system artifacts were excluded automatically from the subsequent ICA on the basis of predefined amplitude thresholds (0.7 pT/cm for planar gradiometers and 3 pT for magnetometers). The ICA decomposition was then performed using the FastICA algorithm (dimension reduction to 30, nonlinearity *tanh*) on the remaining, temporally concatenated epochs (Vigário 1997). Artifactual components were identified using temporal correlations with EOG and ECG signals (correlation thresholds: 0.15) and visual inspection of their spatial topography (number of excluded artifactual components ranged

from 2 to 5 across participants). Finally, the time series of those components were regressed out from the raw, continuous data.

The open source software *Fieldtrip* was then used for further preprocessing (Oostenveld et al. 2011). A common pipeline was applied to generate the evoked responses of interest, which included MEG data epoching (−200 ms to 600 ms post-stimulation onset), automatic epoch rejection (same thresholds as above), low-pass filtering (45 Hz), baseline correction (–150 ms to 0 ms post-stimulus onset), and epoch averaging. Epochs corresponding to standard stimuli and to local deviants were averaged separately.

Resting state data were similarly preprocessed and divided into epochs of same length (i.e., 800 ms), so as to provide surrogate MEG signals needed for the statistical assessment of cEMFs elicited by standards and deviants.

Source reconstruction

Individual MRIs were first segmented using the Freesurfer software (Martinos Center for Biomedical Imaging, Massachusetts, USA). MEG and MRI coordinate systems were co-registered manually using the three anatomical fiducial points for initial estimation and then refined with the head surface points. Then, a source grid (5 mm inter-source distance) built on Montreal Neurological Institute (MNI) brain was deformed onto each participant's brain using a non-linear spatial deformation mapping MNI to participants' brain (Ashburner et al. 1997; Ashburner and Friston 1999)(SPM8, Welcome Trust Centre for Neuroimaging, London, UK). On this basis, the forward model was computed using the one-layer boundary element method implemented in the MNE-C suite (Gramfort et al. 2014) (Martinos Center for Biomedical Imaging, Massachusetts, USA).

Source-level distributed activity was then reconstructed for standard, deviant and resting-state epochs using dynamic statistical parametric mapping (dSPM,(Dale and Sereno

1993). The sensor-space noise covariance was estimated from the baseline and the regularization parameter was set using the prior consistency condition derived in (Wens et al. 2015). The source power time courses were defined as the Euclidian norm of the three components of each dipole.

At the individual level, this data processing and source reconstruction allowed us to determine the location, timing and amplitude of the corresponding cEMFs.

Statistical assessments

Individual level analyses in source space

First, the significance of source-projected cEMFs at primary sensory cortices elicited by standard stimuli in somatosensory and auditory oddballs was evaluated individually, both in FRDA patients and healthy subjects. To do so, we focused on the time interval 0–300 ms post-stimulus onset and investigated the difference between individual cEMFs and the analogous signal derived from resting-state epochs (matched for same epoch length and number) using a non-parametric permutation test. To deal with the issue of multiple spatio-temporal comparisons (16102 sources × 300 time samples), we used a maximum-based unpaired, two-tailed statistic (Nichols and Holmes 2002) built as the maximum absolute difference over all sources and all considered time points. Its null distribution was generated from 1000 random permutations of the conditions (i.e., standard vs. resting-state). The significance threshold at $p < 0.05$ was then derived as the 95^{th} percentile of this distribution. Source-projected cEMFs were deemed statistically significant whenever the maximum statistic exceeded this threshold. In that case, the timeframe of significance was identified as the periods during which the time course of the spatial maximum of differences between standards and resting-state epochs exceeded the above-mentioned threshold, and the spatial localization was obtained as supra-threshold activity within these timeframes. The latency and

the amplitude of the peak of the first cortical response elicited by standards in somatosensory and auditory oddballs were then visually identified within the timeframe of significance for each FRDA patient and healthy subjects. The resulting latencies and maximum amplitudes were compared between FRDA patients and healthy subjects via classical unpaired, two-tailed Student's t tests for each condition (i.e., standards in somatosensory and auditory oddballs).

We subsequently investigated the existence of differences between source-space cEMFs elicited by standards and deviants in somatosensory and auditory oddball paradigms for each FRDA patient and healthy subject. A similar non-parametric maximum-based permutation approach was used to that effect but here, random permutations mixed standard and deviant epochs in each participant and each modality (i.e., somatosensory and auditory oddballs). The location, latency and amplitude of mMMN responses were identified using a similar approach as describe above.

Finally, we examined in FRDA patients the possible relations between brain responses (the maximum amplitude of the first cortical responses elicited by standards in somatosensory and auditory oddballs as well as smMMN and amMMN responses) and patients' characteristics (disease duration, size of GAA1 triplet expansion, and SARA score) using Spearman's rank correlation. In FRDA patients lacking statistically significant standard, smMMN, or amMMN cortical response, we visually identified the maximum response amplitude at the mean location and latency of significant cortical response observed across the individual FRDA patients with significant cortical response.

Group level analyses in source space

The existence of statistically significant difference between the cortical responses elicited by deviants and standards in both tactile and auditory modalities was also examined at the group level in FRDA patients and healthy subjects. The analysis was similar to that used

to derive individual-level statistics. The only difference was that units being permuted were subjects' averaged data in both conditions rather than epochs.

Differences in amMMN and smMMN between FRDA patients and matched healthy subjects were sought using the same statistical scheme. Of note, to avoid significant differences due to delayed responses in FRDA patients, we used a non-parametric approach to test if the latencies of the maximum group-level MMN response were different in healthy subjects and FA patients. To do so, for each of the two groups, the distribution of group-level maximum response timing was estimated using a resampling strategy (number of resamples: 10.000), whereby this latency was obtained from the MMN derived using a random selection of 16 healthy subjects/FRDA patients with replacement. We, then, tested for a significant difference in the mean latency (i.e., difference in the two MMN peak timings) using a permutation test on these two distributions (number of random permutations of healthy subjects/FRDA patients label: 10.000). If there was a significant difference in MMN latencies between groups, the difference between group-level amMMN and smMMN in FRDA patients and healthy subjects was sought after temporal realignment on the timing of group-level maximum MMN response in each modality.

Effects of MEG systems on acquired results

In order to exclude a system (Vectorview vs. Triux) effect on the observed evoked responses, data from healthy subjects were split into one subgroup whose data was acquired with the Vectorview system (7 subjects) and another, with the Triux system (9 subjects). We, then, assessed the system effect by comparing their evoked responses for each sensor and time sample using a two-tailed unpaired t-test. Given the large number of comparisons, we estimated the number of comparisons involved as the product of the number of spatial degrees of freedom (about 80 after signal space separation) and of temporal degrees of freedom (as estimated on the basis of the largest frequency in the data, i.e., 45 Hz) and applied a

Bonferoni correction to the t-tests at $p<0.05$ corrected. Furthermore, to preclude a potential effect induced in our source-level group comparisons by the two MEG system used that may have escaped the statistics of the sensor-space evoked response comparison, source-level statistical tests were re-run by introducing explicitly the MEG system type as a covariate of non-interest so as to eliminate the potential system effect. Specifically, we first regressed the system type out of the evoked responses and then rerun our maximum-based permutation tests

Results

Figure 2 shows butterfly plots of the grand-averaged data for standard and deviant stimuli, and their difference (i.e., MMN) in each sensory modality and participants' group.

Evoked responses to standards in tactile and auditory paradigms

Figure 2 shows a butterfly plot of the grand averaged raw data of standard and deviant stimuli in each modality and groups. Figures 3 and 5 illustrate the latency and the amplitude of source-space standard-elicited tactile (Figure 3) and auditory (Figure 5) cEMFs at primary sensory cortices in FRDA patients and healthy subjects as well as the correlation of the maximum amplitude of those responses with the size of GAA1 triplet expansion in FRDA patients.

Tactile evoked responses (Figure 3)

At the individual level, statistically significant somatosensory cEMFs were found for standards at SI cortex contralateral to stimulation (cSI) in all but one FRDA patients (mean ± SD MNI peak coordinates [-38.5 -24.2 47.3] ± [4.2 7.8 4.1] mm) and in all healthy subjects ([-39.8 -25.2 47.3] ± [5.6 6.4 15.7] mm). Maximum significant cSI cortical responses had longer latencies and smaller amplitudes of peak response in FRDA patients than in healthy subjects (latency, 56.0 ± 20.3 ms vs. 30.3 ms ± 6.0, $p < 0.001$; dSPM amplitude, 0.29 ± 0.17 vs. 0.51 ± 0.18 dSPM, $p = 0.004$). In FRDA patients, the maximum amplitude of cSI cortex response significantly correlated with the size of GAA1 repeat expansion ($R = -0.74$, $p = 0.003$, Spearman correlation), but neither with disease duration ($R = 0.13$, $p = 0.64$), nor with the SARA score ($R = -0.07$, $p = 0.80$).

Of note, a N20 response could be clearly identified in only two of the nine FRDA patients who underwent classical SSEP testing, with latencies of 26.1 ms and 27.65 ms, and

amplitudes of 0.3 μV and 0.38 μV (normal N20 latency 19.6 ± 1.02 ms; normal N20 amplitude 2.1 ± 0.9 μV). Importantly, in addition to the two subjects who displayed N20 responses, six out of the seven patients who did not display clear N20 responses had significant cSI cortex responses in MEG recordings. (Figure 4)

Auditory evoked responses (Figure 5)

Statistically significant auditory cEMFs to unilateral standards were recorded at the contralateral (cAI) and ipsilateral (iAI) auditory cortices in all FRDA patients but one (cAI, [-52.8 -24 5.8] ± [4.1 7.5 5.3] mm; iAI, [54.8 -16.9 3.6] ± [5.4 8.9 5.2] mm), and in all healthy subjects (cAI, [-50.4 -25.4 3.2] ± [3.7 9.0 9.7] mm; iAI, [56.3 -17.4 6.1] ± [1.8 6.5 3.0] mm).

Maximum significant cAI and iAI cortical responses had longer latencies in FRDA patients than in healthy subjects (cAI, 107 ± 23 ms vs. 87 ± 11 ms, $p = 0.011$; iAI, 115 ± 31 ms vs. 96 ± 11 ms, $p = 0.038$), but there were no significant differences in dSPM amplitude (cAI, 0.55 ± 0.29 vs. 0.42 ± 0.23, $p = 0.51$; iAI, 0.5 ± 0.3 vs. 0.3 ± 0.12, $p = 0.13$).

In FRDA patients, the maximum amplitude of the cAI response to standards negatively correlated with the size of GAA1 repeat expansion ($R = -0.56$, $p = 0.036$), but neither with disease duration ($R = 0.14$, $p = 0.64$), nor with the SARA score ($R = -0.34$, p = 0.23). Conversely, there was no correlation between the maximum amplitude of the iAI response to standards and the size of GAA1 repeat expansion ($R = -0.3$, $p = 0.29$), the SARA score (-0.15, $p = 0.57$) or disease duration ($R = -0.3$, $p = 0.24$).

Early neocortical sensory change detection

Figures 6 and 7 illustrate smMMN (Figure 6) and amMMN (Figure 7) responses obtained in FRDA patients and in healthy subjects as well as the correlation of the maximum amplitude of smMMN responses with the size of GAA1 triplet expansion in FRDA patients.

Early cortical somatosensory change detection

In 11/16 healthy subjects, a significant smMMN was recorded only at cSII cortex from 83 ± 30 ms to 132 ± 28 ms post-deviant onset (peak difference [-43.0 -25.3 28.0] mm ± [4.6 7.4 7.0] mm, dSPM amplitude difference 0.62 ±0.3). At the group level, a significant smMMN was found only at cSII cortex ([-46 -25 24] mm, amplitude: 0.5 dSPM unit) from 63 to 139 ms post-deviant onset.

In 6/16 FRDA patients, a significant smMMN was also detected only at cSII cortex from 117 ± 41 ms to 151 ± 16.4 ms post-deviant onset ([-46.8 -16.2 16.7] mm ± [7.9 8.4 7.0] mm, 0.38 ± 0.21 dSPM unit). Patients with significant smMMN had a GAA1 of 650 ± 264 triplet expansions, an age of onset of 15.6 ± 7.6, a disease duration of 20.1 ± 9.7 and a mean SARA score of 24.2 ± 7.3. Of note, no significant difference was found, with a T-test, between FRDA patients with and without significant smMMN in their size of GAA1 triplet expansion (650 ± 264 vs. 771± 166, p = 0.13), age of onset (15.6 y ± 7.6 vs. 11.8 y ± 4.3, p = 0.11), disease duration (20.1 y ± 9.7 vs. 15.6 ± 10.2, p = 0.18) and mean SARA score (24.2 ± 7.3 vs. 25.6 ± 6.8, p = 0.35).

At the group level, a significant smMMN was found only at cSII cortex ([-49 -19 19] mm, 0.2 dSPM unit) from 114 to 170 ms post-deviant onset.

The resampling analysis showed that smMMN peak occurred significantly later in FRDA patients than in healthy subjects (mean increased latency in FRDA patients: 40 ms; $p <$ 0,001). Therefore, smMMN responses were temporally realigned based on the timing of the maximum cSII cortex response to allow proper source space comparison between FRDA patients and healthy subjects. A significantly higher smMMN response at cSII cortex ([-40 -25 30] mm, dSPM amplitude difference 0.4) was observed in healthy subjects compared with FRDA patients from 73 to 122 ms post-deviant onset.

In FRDA patients, the smMMN amplitude at cSII cortex correlated significantly with the size of GAA1 repeat expansion (n = 15; R = -0.65, p = 0.0082) but neither with disease duration (n = 16; R = 0.23, p = 0.40), nor with the SARA score (n = 16; R = -0.18, p = 0.51).

Early neocortical auditory change detection

In 10/16 healthy subjects, a significant amMMN was detected 161 ± 33 ms to 190 ± 43 ms post-deviant onset at cAI ([-49.8 -14.2 4.3] mm ± [6.8 8.7 7.8] mm, 0.42 ± 0.18 dSPM unit) and iAI ([54.3 -19.7 3.8] mm ± [3.4 18.5 2.2] mm, 0.4 ± 0.1 dSPM unit) cortices. At the group level, a significant amMMN response was found only at the cAI cortex ([-40 -22 9] mm, 0.11 dSPM unit) from 162 to 172 ms after deviants onset.

In 11/16 FRDA patients, a significant amMMN was detected 164 ± 26 ms to 189 ± 23 ms post-deviant onset at cAI ([-46.7 -22.5 7.7] mm ± [5.3 4.8 1.8] mm, 0.44 ± 0.18 dSPM unit) and iAI ([53.2 -16.9 2.4] mm ± [5.8 8.0 3.9] mm, 0.34 ±0.1 dSPM unit) cortices. At the group level, a significant amMMN was also found only at cAI cortex ([-43 -19 6] mm, 0.2 dSPM unit) from 150 to 180 ms after deviant onset.

The resampling analysis disclosed no latency differences in amMMN between FRDA and healthy subjects. Therefore, no temporal realignment of amMMN responses was performed to search for differences in amMMN response amplitude. No difference in amMMN amplitude was found between FRDA patients and healthy subjects.

Effect of the MEG systems on evoked magnetic fields

No significant difference was found between healthy subjects' sensor-level evoked response obtained with the two MEG systems. At the source-level, after regressing out the potential effects of the MEG system from the data, results were quantitatively similar and none of our conclusions affected, excluding that the results are driven by the type of MEG system used.

Discussion

This MEG study conducted in a large population of genetically proven FRDA patients demonstrates that (i) tactile and auditory standard stimuli elicit robust but abnormal responses at cSI (delayed and reduced in amplitude) and AI (only delayed) cortices respectively in FRDA patients compared with healthy controls, (ii) early neocortical sensory change detection is altered in FRDA-patients for the tactile modality but not for the auditory modality, and (iii) the amplitude of the smMMN response at cSII cortex correlates with the size of GAA1 repeat expansion but not with disease duration nor severity. Taken together, these data bring empirical evidence supporting the contribution of cerebellar pathways in smMMN genesis at cSII cortex.

Neuromagnetic evoked responses to standards and deviants in healthy subjects

Brain responses recorded in healthy controls peaked at timings and locations compatible with previous reports. In all healthy subjects, standard tactile stimuli elicited a significant cortical response at the post-central gyrus contralateral to the stimulation, corresponding to SI cortex in terms of MNI coordinates (Pleger et al. 2003; Eickhoff et al. 2005) and latency (Mauguiere et al. 1997; Hari and Forss 1999; Papadelis et al. 2011; Avanzini et al. 2016). Similarly, standard auditory stimuli elicited significant cortical responses typical of bilateral AI cortex in terms of MNI coordinates (Rademacher et al. 2001) and timing (Virtanen et al. 1998). Significant smMMN and amMMN responses were found in two-third of healthy subjects, which corresponds to the rate reported at the subject level in previous studies on smMMN (Naeije et al. 2016) and amMMN (Faugeras et al. 2012; King et al. 2013; Recasens and Uhlhaas 2017). The cortical generator of the smMMN identified using distributed source modeling was located at the first cytoarchitectonic subdivision of the parietal operculum (OP1) as described by Eickhoff's probabilistic maps (Eickhoff et al. 2006)

with regards to right hand somatotopy (Eickhoff *et al.,* 2007). The finding of bilateral AI cortical generators of the amMMN at individual level is also in agreement with previous studies (Hari et al. 1992; Alho et al. 1998; Wacongne et al. 2011). However, at the group level, amMMN was only significant over the left AI cortex, which is in agreement with the fact that in mono-aural auditory oddballs, the amplitude of the aMMN is typically higher on the contralateral side to the stimulation (Chennu et al. 2013; Phillips et al. 2015, 2016). Finally, the timing of smMMN and amMMN responses was in agreement with previous reports (Garrido et al. 2009; Naatanen et al. 2011; Naeije et al. 2016, 2017).

Neuromagnetic evoked responses to tactile standard stimuli and SSEPs in FRDA patients

Results of the present study suggest that MEG is more sensitive than SSEPs, as 6/7 FRDA patients who did not display a N20 potential on SSEPs had significant magnetic cSI cortical responses to tactile standard stimuli. In previous reports, SSEPs could not be recorded in 33 to 68% of FRDA patients (Jones et al. 1980; Pelosi et al. 1984; Vanasse et al. 1988; Santoro et al. 1999, 2000; Santiago-Perez et al. 2007). It is intriguing how the frequent lack of recordable SSEPs in FRDA patients contrasts with their almost normal conscious perception of touch, even if their proprioception is altered (Saunders., 1913). In line with this observation, all patients were able to perceive and discriminate the different tactile stimuli (i.e., standards and deviants), which, along with the fact that neuromagnetic cSI cortex responses were recorded using 500 tactile standard stimuli in all but one FRDA patients, suggests that traditional SSEPs are probably less effective to assess the somatosensory system function in FRDA patients than MEG. The better sensitivity of MEG may be due to various and non-exclusive factors: higher sensors number (306 sensors for MEG vs. eight scalp electrodes for SSEP), better signal to noise ratio for focal neocortical sources and heightened sensitivity to tangential neocortical sources such as area 3b of SI cortex (Goldenholz et al.

2009) that are the primary cortical area for tactile processing (Keysers et al. 2010). Furthermore, in this study, we used pneumatic tactile stimuli that may recruit smaller caliber, less affected nerve fibers than electrical stimuli (Forss et al. 1994). Overall, our results indicate that MEG is a sensitive tool to study cortical sensory processing in diseases affecting the afferent sensory pathways such as FRDA.

FRDA patients displayed longer latencies and smaller amplitudes than control subjects for the maximal response elicited by tactile standard stimuli at cSI cortex. Increased latency of cSI cortex responses elicited by tactile stimuli is easily explained by the selective loss of large-size fast-conducting primary somatosensory neurons in the DRGs, along with their peripheral and central axonal branches in sensory nerves and in the posterior columns of the spinal cord (Hughes et al. 1968; Zouari et al. 1998; Santoro et al. 1999; Santiago-Perez et al. 2007). Prolonged somatosensory central conduction time is well described in various diseases affecting the posterior columns of the spinal cord, such as multiple sclerosis (Ganes 1980), vitamin B12 deficiency (Zegers de Beyl et al. 1988), stroke (Tinazzi and Mauguiere 1995) and medullary compression (Miyoshi and Kimura 1996), in addition to FRDA (Santiago-Perez et al. 2007). The decrease in cSI cortex responses amplitude to tactile standard stimuli might be due to sensory neuron loss, but also to cerebellar pathology. Indeed, patients with unilateral cerebellar lesions (Restuccia et al. 2001)have smaller SI cortex responses to tactile stimuli on the ipsilateral hand to the cerebellar lesions and, in animal studies, induced cerebellar lesions lead to altered SI cortex responses (Kolodziejak et al. 2000). However, our results suggest that afferent pathology is mainly responsible for the loss of amplitude of SI cortex responses in FRDA patients. Indeed, as in a previous SSEPs study (Santoro et al. 2000), the maximum amplitude of tactile cEMFs at cSI cortex correlated with the size of GAA1 repeat expansion, but not with the SARA score, nor with the disease duration. Cerebellar degeneration progressively occurs along the course of the disease in FRDA

(Koeppen and Mazurkiewicz 2013; Silva et al. 2013; Koeppen et al. 2016; Rezende et al. 2016). So, a decrease in the amplitude of the cSI cortex response due to cerebellar degeneration should correlate with the SARA score that mainly reflects cerebellar progressive structural and functional alterations (Akhlaghi et al. 2011; Silva et al. 2013; Selvadurai et al. 2016) or disease duration, which was not the case. The observed correlation with the size of GAA1 triplet expansion instead suggests that the reduction in cSI cortex responses mostly depends on lemniscal pathway atrophy, already present at disease onset (Said et al. 1986; Santoro et al. 1999), mostly developmental (Ouvrier et al. 1982; Santoro et al. 1999), and whose extent is mostly determined by the severity of the trinucleotide repeat expansion.

Neuromagnetic evoked responses to auditory standard stimuli in FRDA patients

Auditory perception is affected in FRDA patients at all levels of processing, from brainstem to early and late cortical sound/speech processing (Al-Azzawi and Mirza 2004; Rance et al. 2008, 2012). Yet, most studies in FRDA concentrated on brainstem auditory evoked potentials (BAEPs) and consistently showed that they are either absent or delayed (Pedersen and Trojaborg 1981; Taylor et al. 1982; Jabbari et al. 1983; Taylor 1983; Amantini et al. 1984; Campanella et al. 1984; Ell et al. 1984; De Pablos et al. 1991; Caruso et al. 1992). Cortically generated middle latency responses (MLR) (Onitsuka et al. 2003) and the more prominent long latency responses (LLR) (Virtanen et al. 1998) have been seldom studied in FRDA and, to the best of our knowledge, not since genetic testing became widely available. In clinically diagnosed FRDA patients, MLR and LLR responses were found to be delayed or absent (Shanon et al. 1981; Taylor et al. 1982; Amantini et al. 1984). In the present study, auditory cortical LLR elicited by auditory standard stimuli were present in all but one FRDA patients but were significantly delayed compared with healthy controls while their maximum amplitude was not different. The maximal amplitude of cAI cortex evoked responses to

auditory standard stimuli negatively correlated with the size of GAA1 repeat expansion but not with the SARA score nor the disease duration (Satya-Murti et al. 1980; Santoro et al. 1999).

Taken together, these observations support the view that both somatosensory and auditory pathways are affected early in the disease, in a genetically determined fashion that does not substantially evolve with disease progression.

Early tactile change detection is impaired in FRDA and correlates with the size of GAA1 triplet repeat expansion

Only 37% of FRDA patients displayed significant smMMN at cSII cortex, compared to 69% of healthy controls, and with smaller amplitude. A first explanation for the lower smMMN amplitude could be the loss of somatosensory afferences, as shown by lower cSI cortex responses to tactile standard stimuli. However, while responses at cSI and cSII cortices are related, their relation is complex and not strictly hierarchical, with parallel rather than serial processing of somatosensory stimuli (Karhu and Tesche 1999; Simoes et al. 2002; Gao et al. 2015). In a previous MEG study, pneumatic tactile stimuli applied to the proximal phalange of the middle finger elicited cSI cortex responses of at least 44% of the magnitude of those elicited by electrical median nerve stimulation slightly above motor threshold (Forss et al. 1994). However, in that study, cSII cortex responses were comparable between pneumatic and electrical stimuli, indicating that the magnitude of cSII cortex responses neither depends directly on the amount of stimulated afferent fibers, nor on the amplitude of the cSI cortex response (Forss et al. 1994). Indeed, the amplitude of cSII cortex responses is more influenced by the stimulus rate than stimulus intensity (Wikstrom et al. 1996; Naeije et al. 2017). Additionally, cSII cortex responses are well described in the absence of any cSI cortex response, like in off-responses (Yamashiro et al. 2008; Otsuru et al. 2011) and

omission paradigms (Yamashiro et al. 2008, 2009; Naeije et al. 2017; Andersen and Lundqvist 2019). Finally, cSII cortex responses were similar in patients with reduced cSI cortex responses due to thalamic lesions compared with healthy subjects (Taskin et al. 2006) and in a primate models in which the inactivation of cSI cortex by cooling did not lead to subsequent cSII disappearance arguing for parallel processing of tactile stimuli at cSI and cSII (Zhang et al. 1996). Therefore, the 40% mean reduction in magnitude of cSI cortex responses to tactile standard stimuli in all but one of our FRDA patients should not *per se* lead to reduced or absent cSII cortex responses. If afferent loss cannot convincingly explain reduced smMMN at cSII cortex in FRDA, cerebellar impairment of tactile processing might be involved. In this regard, our findings in FRDA patients parallel observations in healthy subjects who underwent cerebellar inhibition by tDCS and showed reduced sMMN responses (Chen et al. 2014), and in patients with unilateral cerebellar lesions who displayed almost no sMMN response after the presentation of deviant somatosensory stimuli on the hand ipsilateral to the affected cerebellar hemisphere (Restuccia et al. 2007). The use of unilateral stimuli in our study could have biased the results if cerebellar and afferent disorders in FRDA were asymmetrical. However, symptoms in FRDA are comparable and highly correlated between right and left hands on clinical scales. Furthermore, alterations on structural and functional neuroimaging as well as on pathology are typically symmetrical(Dürr et al. 1996; Subramony et al. 2005; Akhlaghi et al. 2011; Koeppen and Mazurkiewicz 2013; Zalesky et al. 2014; Vavla et al. 2018). These findings therefore render a laterality bias in our results unlikely. By contrast, the amMMN was similar in healthy subjects and in FRDA patients. This lack of difference in amMMN responses parallels previous work on healthy subjects where cerebellar inhibition by tDCS did not alter aMMN responses (Chen et al. 2014)), and studies on acquired and degenerative cerebellar lesions where patients had preserved pitch aMMN (Restuccia et al. 2007; Moberget et al. 2008). In FRDA patients, tactile change

detection alterations negatively correlated with the size of GAA1 triplet expansion. This suggests the involvement of an afferent cerebellar pathways impairment due to diminished input from atrophied spinocerebellar and cuneocerebellar tracts that would result from primary somatosensory neurons and dorsal column pathology through trans-neuronal ascending degeneration (i.e., degeneration of spinocerebellar and cuneocerebellar tracts neurons due to a lack of input from first-order somatosensory neurons (Koeppen and Mazurkiewicz 2013). Indeed, lack of correlation with the SARA or disease duration indicates that alteration of efferent cerebellar pathways due to dentate pathology is less likely contributing to altered tactile change detection at cSII cortex (Silva et al. 2013). Still, a role of the indirect afferent pathway due to impaired cortico-ponto-cerebellar tracts also cannot be totally excluded.

Conclusions

This study demonstrates that, in FRDA, tactile evoked responses are delayed and reduced in amplitude at cSI cortex while auditory evoked responses are only delayed at AI cortices. Furthermore, it shows that smMMN responses at cSII cortex are impaired in FRDA patients while amMMN responses are preserved. Maximal amplitudes of tactile evoked, auditory evoked and smMMN responses do correlate with the genotype but not with clinical parameters. Overall, this study demonstrates a distinctive effect of FRDA pathology on somatosensory and auditory systems, as previously reported in patients with cerebellar disorders.

Conflicts of interests:

No authors report any conflict of interests

Acknowledgments

This study was financially supported by (i) the research grant "Les Voies du Savoir" from the Fonds Erasme (Brussels, Belgium) and (ii) the Fonds de la Recherche Scientifique (FRS-FNRS, Brussels, Belgium; research credit: J.0095.16.F). Gilles Naeije was supported by a research grant from the Fonds Erasme (Brussels, Belgium). Mathieu Bourguignon was supported by the program Attract of Innoviris (grant 2015-BB2B-10), by the Spanish Ministry of Economy and Competitiveness (grant PSI2016-77175-P), and by the Marie Skłodowska-Curie Action of the European Commission (grant 743562). Xavier De Tiège is Postdoctorate Clinical Master Specialist at the Fonds de la Recherche Scientifique (FRS-FNRS, Brussels, Belgium). The MEG project at the CUB Hôpital Erasme is financially supported by the Fonds Erasme (Research grant "Les Voies du Savoir", Brussels, Belgium).

The authors would like to thank Brice Marty for his help in MEG data acquisition.

References

Akatsuka K, Wasaka T, Nakata H, Inui K, Hoshiyama M, Kakigi R. Mismatch responses related to temporal discrimination of somatosensory stimulation. Clin Neurophysiol. 2005;116(8):1930–7.

Akhlaghi H, Corben L, Georgiou-Karistianis N, Bradshaw J, Storey E, Delatycki MB, et al. Superior cerebellar peduncle atrophy in Friedreich's ataxia correlates with disease symptoms. Cerebellum. 2011;10(1):81–7.

Al-Azzawi LM, Mirza KB. The usefulness of the brainstem auditory evoked potential in the early diagnosis of cranial nerve neuropathy associated with diabetes mellitus. Electromyogr Clin Neurophysiol. 2004;44(7):387–94.

Alho K, Winkler I, Escera C, Huotilainen M, Virtanen J, Jääskeläinen IP, et al. Processing of novel sounds and frequency changes in the human auditory cortex:

magnetoencephalographic recordings. Psychophysiology. 1998;35(2):211–24.

Amantini A, Rossi L, De Scisciolo G, Bindi A, Pagnini P, Zappoli R. Auditory evoked potentials (early, middle, late components) and audiological tests in Friedreich's ataxia. Electroencephalogr Clin Neurophysiol. 1984;58(1):37–47.

Andersen LM, Lundqvist D. Somatosensory responses to nothing: An MEG study of expectations during omission of tactile stimulations. Neuroimage. 2019;184:78–89.

Ashburner J, Friston KJ. Nonlinear spatial normalization using basis functions. Hum Brain Mapp. 1999;7(4):254–66.

Ashburner J, Neelin P, Collins DL, Evans A, Friston K. Incorporating Prior Knowledge into Image Registration. Neuroimage. 1997;6(4):344–52.

Avanzini P, Abdollahi RO, Sartori I, Caruana F, Pelliccia V, Casaceli G, et al. Four-dimensional maps of the human somatosensory system. Proc Natl Acad Sci. 2016;113(13):E1936–43.

Baumann O, Borra RJ, Bower JM, Cullen KE, Habas C, Ivry RB, et al. Consensus paper: the role of the cerebellum in perceptual processes. Cerebellum. 2015;14(2):197–220.

Bekinschtein TA, Dehaene S, Rohaut B, Tadel F, Cohen L, Naccache L. Neural signature of the conscious processing of auditory regularities. Proc Natl Acad Sci. 2009;106(5):1672–7.

Campanella G, De Falco FA, Santoro L, Perretti A, Cassandro E, Mosca F. Specific impairment of BAER's in Friedreich's ataxia. Auditory evoked responses in clinical evaluation and differential diagnosis. J Neurol Sci. 1984;65(1):111–20.

Campuzano V, Montermini L, Molto MD, Pianese L, Cossee M, Cavalcanti F, et al. Friedreich's ataxia: autosomal recessive disease caused by an intronic GAA triplet repeat expansion. Science. 1996;271(5254):1423–7.

Caruso G, Santoro L, Perretti A. Clinical and electrophysiological findings in various

hereditary sensory neuropathies. Acta Neurol (Napoli). 1992;14(4–6):345–62.

Chen J-C, Hämmerer D, D'Ostilio K, Casula EP, Marshall L, Tsai C-H, et al. Bi-directional modulation of somatosensory mismatch negativity with transcranial direct current stimulation: an event related potential study. J Physiol. 2014;592(4):745–57.

Chennu S, Noreika V, Gueorguiev D, Blenkmann A, Kochen S, Ibanez A, et al. Expectation and Attention in Hierarchical Auditory Prediction. J Neurosci. 2013;33(27):11194–205.

Clark VP, Fannon S, Lai S, Benson R, Bauer L. Responses to rare visual target and distractor stimuli using event-related fMRI. J Neurophysiol. 2000;83(5):3133–9.

Czigler I, Balázs L WI. Memory-based detection of task-irrelevant visual changes. - PubMed - NCBI. Psychophysiology. 2002;39(6):869–73.

Dale AM, Sereno MI. Improved Localizadon of Cortical Activity by Combining EEG and MEG with MRI Cortical Surface Reconstruction: A Linear Approach. J Cogn Neurosci. 1993;5(2):162–76.

Downar J, Crawley AP, Mikulis DJ, Davis KD. A multimodal cortical network for the detection of changes in the sensory environment. Nat Neurosci. 2000;3(3):277–83.

Dürr A, Cossee M, Agid Y, Campuzano V, Mignard C, Penet C, et al. Clinical and Genetic Abnormalities in Patients with Friedreich's Ataxia. N Engl J Med. 1996;335(16):1169–75.

Eickhoff SB, Schleicher A, Zilles K, Amunts K. The human parietal operculum. I. Cytoarchitectonic mapping of subdivisions. Cereb Cortex. 2006;16(2):254–67.

Eickhoff SB, Stephan KE, Mohlberg H, Grefkes C, Fink GR, Amunts K, et al. A new SPM toolbox for combining probabilistic cytoarchitectonic maps and functional imaging data. Neuroimage. 2005;25(4):1325–35.

Ell J, Prasher D, Rudge P. Neuro-otological abnormalities in Friedreich's ataxia. J Neurol Neurosurg Psychiatry. 1984 Jan;47(1):26–32.

Faugeras F, Rohaut B, Weiss N, Bekinschtein T, Galanaud D, Puybasset L, et al. Event related potentials elicited by violations of auditory regularities in patients with impaired consciousness. Neuropsychologia. 2012;50(3):403–18.

Forss N, Salmelin R, Hari R. Comparison of somatosensory evoked fields to airpuff and electric stimuli. Electroencephalogr Clin Neurophysiol. 1994;92(6):510–7.

Friedreich N. Ueber degenerative Atrophie der spinalen Hinterstränge. Arch für Pathol Anat und Physiol und für Klin Med. 1863;26(5–6):433–59.

Ganes T. Somatosensory evoked responses and central afferent conduction times in patients with multiple sclerosis. J Neurol Neurosurg Psychiatry. 1980;43(10):948–53.

Gao L, Sommerlade L, Coffman B, Zhang T, Stephen JM, Li D, et al. Granger causal time-dependent source connectivity in the somatosensory network. Sci Rep. 2015;5(1):10399.

Garrido MI, Kilner JM, Stephan KE, Friston KJ. The mismatch negativity: A review of underlying mechanisms. Clin Neurophysiol. 2009;120(3):453–63.

Goldenholz DM, Ahlfors SP, Hämäläinen MS, Sharon D, Ishitobi M, Vaina LM, et al. Mapping the signal-to-noise-ratios of cortical sources in magnetoencephalography and electroencephalography. Hum Brain Mapp. 2009;30(4):1077–86.

González-Cabo P, Palau F. Mitochondrial pathophysiology in Friedreich's ataxia. J Neurochem . 2013;126 Suppl 1:53–64.

Gramfort A, Luessi M, Larson E, Engemann DA, Strohmeier D, Brodbeck C, et al. MNE software for processing MEG and EEG data. Neuroimage. 2014;86:446–60.

Hari R, Forss N. Magnetoencephalography in the study of human somatosensory cortical processing. Philos Trans R Soc B Biol Sci. 1999;354(1387):1145–54.

Hari R, Rif J, Tiihonen J, Sams M. Neuromagnetic mismatch fields to single and paired tones. Electroencephalogr Clin Neurophysiol. 1992;82(2):152–4.

Hughes JT, Brownell B, Hewer RL. The peripheral sensory pathway in friedreich's ataxia. An

examination by light and electron microscopy of the posterior nerve roots, posterior root ganglia, and peripheral sensory nerves in cases of friedreich's ataxia. Brain. 1968;91(4):803–18.

Hunold A, Funke ME, Eichardt R, Stenroos M, Haueisen J. EEG and MEG: sensitivity to epileptic spike activity as function of source orientation and depth. Physiol Meas. 2016;37(7):1146–62.

Jabbari B, Schwartz DM, MacNeil DM, Coker SB. Early abnormalities of brainstem auditory evoked potentials in Friedreich's ataxia: evidence of primary brainstem dysfunction. Neurology. 1983;33(8):1071–4.

Jones SJ, Baraitser M, Halliday AM. Peripheral and central somatosensory nerve conduction defects in Friedreich's ataxia. J Neurol Neurosurg Psychiatry. 1980;43(6):495–503.

Karhu J, Tesche CD. Simultaneous Early Processing of Sensory Input in Human Primary (SI) and Secondary (SII) Somatosensory Cortices. J Neurophysiol. 1999;81(5):2017–25.

Kekoni J, Hämäläinen H, Saarinen M, Gröhn J, Reinikainen K, Lehtokoski A, et al. Rate effect and mismatch responses in the somatosensory system: ERP-recordings in humans. Biol Psychol . 1997;46(2):125–42.

Keysers C, Kaas JH, Gazzola V. Somatosensation in social perception. Nat Rev Neurosci. 2010;11(6):417–28.

King JR, Faugeras F, Gramfort A, Schurger A, El Karoui I, Sitt JD, et al. Single-trial decoding of auditory novelty responses facilitates the detection of residual consciousness. Neuroimage. 2013;83:726–38.

Koeppen AH, Mazurkiewicz JE. Friedreich Ataxia: Neuropathology Revised. J Neuropathol Exp Neurol. 2013;72(2):78–90.

Koeppen AH, Ramirez RL, Becker AB, Mazurkiewicz JE. Dorsal root ganglia in Friedreich ataxia: satellite cell proliferation and inflammation. Acta Neuropathol Commun.

2016;4(1):46.

Kolodziejak A, Dziduszko J, Niechaj A, Tarnecki R. Influence of acute cerebellar lesions on somatosensory evoked potentials (SEPs) in cats. J Physiol Pharmacol. 2000;51(1):41–55.

Kotz SA, Stockert A, Schwartze M. Cerebellum, temporal predictability and the updating of a mental model. Philos Trans R Soc Lond B Biol Sci. 2014;369(1658):20130403.

Leggio M, Molinari M. Cerebellar sequencing: a trick for predicting the future. Cerebellum. 2015;14(1):35–8.

Mascalchi M, Bianchi A, Ciulli S, Ginestroni A, Aiello M, Dotti MT, et al. Lower medulla hypoplasia in Friedreich ataxia: MR Imaging confirmation 140 years later. Vol. 264, Journal of neurology. Germany; 2017. p. 1526–8.

Mauguiere F, Merlet I, Forss N, Vanni S, Jousmaki V, Adeleine P, et al. Activation of a distributed somatosensory cortical network in the human brain: a dipole modelling study of magnetic fields evoked by median nerve stimulation. Part II: Effects of stimulus rate, attention and stimulus detection. Electroencephalogr Clin Neurophysiol. 1997;104(4):290–5.

Miyoshi T, Kimura J. Short-latency somatosensory evoked potentials in patients with cervical compressive lesions: morphological versus functional examination. Electromyogr Clin Neurophysiol. 1996;36(6):323–32.

Moberget T, Karns CM, Deouell LY, Lindgren M, Knight RT, Ivry RB. Detecting violations of sensory expectancies following cerebellar degeneration: a mismatch negativity study. Neuropsychologia. 2008;46(10):2569–79.

Naatanen R, Alho K. Generators of electrical and magnetic mismatch responses in humans. Brain Topogr. 1995;7(4):315–20.

Naatanen R, Kujala T, Kreegipuu K, Carlson S, Escera C, Baldeweg T, et al. The mismatch negativity: an index of cognitive decline in neuropsychiatric and neurological diseases

and in ageing. Brain. 2011;134(Pt 12):3435–53.

Naeije G, Vaulet T, Wens V, Marty B, Goldman S, De Tiège X. Multilevel cortical processing of somatosensory novelty: A magnetoencephalography study. Front Hum Neurosci. 2016;10.

Naeije G, Vaulet T, Wens V, Marty B, Goldman S, De Tiège X, et al. Neural basis of early somatosensory change detection: a magnetoencephalography study. Brain Topogr. 2017;31(2):242–56.

Nichols TE, Holmes AP. Nonparametric permutation tests for functional neuroimaging: A primer with examples. Hum Brain Mapp. 2002;

Onitsuka T, Ninomiya H, Sato E, Yamamoto T, Tashiro N. Differential characteristics of the middle latency auditory evoked magnetic responses to interstimulus intervals. Clin Neurophysiol. 2003;114(8):1513–20.

Oostenveld R, Fries P, Maris E, Schoffelen JM. FieldTrip: Open source software for advanced analysis of MEG, EEG, and invasive electrophysiological data. Comput Intell Neurosci. 2011:156869.

Otsuru N, Inui K, Yamashiro K, Urakawa T, Keceli S, Kakigi R. Effects of prior sustained tactile stimulation on the somatosensory response to the sudden change of intensity in humans: an magnetoencephalography study. Neuroscience. 2011;182:115–24.

Ouvrier RA, McLeod JG, Conchin TE. Friedreich's ataxia. Early detection and progression of peripheral nerve abnormalities. J Neurol Sci. 1982;55(2):137–45.

De Pablos C, Berciano J, Calleja J. Brain-stem auditory evoked potentials and blink reflex in Friedreich's ataxia. J Neurol. 1991;238(4):212–6.

Pandolfo M. Friedreich Ataxia. Arch Neurol. 2008;65(10). Available from: http://dx.doi.org/10.1001/archneur.65.10.1296

Papadelis C, Eickhoff SB, Zilles K, Ioannides AA. BA3b and BA1 activate in a serial fashion

after median nerve stimulation: direct evidence from combining source analysis of evoked fields and cytoarchitectonic probabilistic maps. Neuroimage. 2011;54(1):60–73.

Pedersen L, Trojaborg W. Visual, auditory and somatosensory pathway involvement in hereditary cerebellar ataxia, Friedreich's ataxia and familial spastic paraplegia. Electroencephalogr Clin Neurophysiol. 1981;52(4):283–97.

Pelosi L, Fels A, Petrillo A, Senatore R, Russo G, Lönegren K, et al. Friedreich's ataxia: clinical involvement and evoked potentials. Acta Neurol Scand . 1984;70(5):360–8.

Phillips HN, Blenkmann A, Hughes LE, Bekinschtein TA, Rowe JB. Hierarchical Organization of Frontotemporal Networks for the Prediction of Stimuli across Multiple Dimensions. J Neurosci. 2015;35(25):9255–64.

Phillips HN, Blenkmann A, Hughes LE, Kochen S, Bekinschtein TA, Cam C, et al. Convergent evidence for hierarchical prediction networks from human electrocorticography and magnetoencephalography. Cortex. 2016;82:192–205.

Pleger B, Foerster AF, Ragert P, Dinse HR, Schwenkreis P, Malin JP, et al. Functional imaging of perceptual learning in human primary and secondary somatosensory cortex. Neuron. 2003;40(3):643–53.

Puce A, Hamalainen MS. A Review of Issues Related to Data Acquisition and Analysis in EEG/MEG Studies. Brain Sci. 2017;7(6).

Rademacher J, Morosan P, Schormann T, Schleicher A, Werner C, Freund HJ, et al. Probabilistic mapping and volume measurement of human primary auditory cortex. Neuroimage. 2001;13(4):669–83.

Rance G, Corben LA, Delatycki MB. Auditory pathway changes mirror overall disease progress in individuals with Friedreich ataxia. Vol. 259, Journal of neurology. Germany; 2012. p. 2746–8.

Rance G, Fava R, Baldock H, Chong A, Barker E, Corben L, et al. Speech perception ability

in individuals with Friedreich ataxia. Brain. 2008;131(Pt 8):2002–12.

Recasens M, Uhlhaas PJ. Test-retest reliability of the magnetic mismatch negativity response to sound duration and omission deviants. Neuroimage. 2017;157:184–95.

Restuccia D, Della Marca G, Valeriani M, Leggio MG, Molinari M. Cerebellar damage impairs detection of somatosensory input changes. A somatosensory mismatch-negativity study. Brain. 2007;130(Pt 1):276–87.

Restuccia D, Valeriani M, Barba C, Le Pera D, Capecci M, Filippini V, et al. Functional changes of the primary somatosensory cortex in patients with unilateral cerebellar lesions. Brain. 2001;124(Pt 4):757–68.

Rezende TJR, Silva CB, Yassuda CL, Campos BM, D'Abreu A, Cendes F, et al. Longitudinal magnetic resonance imaging study shows progressive pyramidal and callosal damage in Friedreich's ataxia. Mov Disord. 2016;31(1):70–8.

Ruano L, Melo C, Silva MC, Coutinho P. The Global Epidemiology of Hereditary Ataxia and Spastic Paraplegia: A Systematic Review of Prevalence Studies. Neuroepidemiology. 2014;42(3):174–83.

Said G, Marion M-H, Selva J, Jamet C. Hypotrophic and dying-back nerve fibers in Friedreich's ataxia. Neurology. 1986;36(10):1292.

Santiago-Perez S, Perez-Conde MC, Ugalde-Canitrot A, Lopez-Pajares MR. A neurophysiological study of the alterations to the central and peripheral nervous systems in Friedreich's ataxia. Rev Neurol. 2007;44(4):193–7.

Santoro L, De Michele G, Perretti A, Crisci C, Cocozza S, Cavalcanti F, et al. Relation between trinucleotide GAA repeat length and sensory neuropathy in Friedreich's ataxia. J Neurol Neurosurg Psychiatry. 1999;66(1):93–6.

Santoro L, Perretti A, Lanzillo B, Coppola G, De Joanna G, Manganelli F, et al. Influence of GAA expansion size and disease duration on central nervous system impairment in

Friedreich's ataxia: contribution to the understanding of the pathophysiology of the disease. Clin Neurophysiol. 2000;111(6):1023–30.

Satya-Murti S, Cacace A, Hanson P. Auditory dysfunction in Friedreich ataxia: result of spiral ganglion degeneration. Neurology. 1980;30(10):1047–53.

Saunders. SENSORY CHANGES IN FRIEDREICH'S DISEASE. Brain. 1913;36:166–72.

Schulz JB, Boesch S, Burk K, Durr A, Giunti P, Mariotti C, et al. Diagnosis and treatment of Friedreich ataxia: a European perspective. Nat Rev Neurol. 2009;5(4):222–34.

Selvadurai LP, Harding IH, Corben LA, Stagnitti MR, Storey E, Egan GF, et al. Cerebral and cerebellar grey matter atrophy in Friedreich ataxia: the IMAGE-FRDA study. J Neurol. 2016;263(11):2215–23.

Shanon E, Himelfarb MZ, Gold S. Auditory function of Friedreich's ataxia. Electrophysiologic study of a family. Arch Otolaryngol. 1981;107(4):254–6.

Silva CB da, Yasuda CL, D'Abreu A, Cendes F, Lopes-Cendes I, Franca MCJ. Neuroanatomical correlates of depression in Friedreich's ataxia: a voxel-based morphometry study. Cerebellum. 2013;12(3):429–36.

Simoes C, Alary F, Forss N, Hari R. Left-hemisphere-dominant SII activation after bilateral median nerve stimulation. Neuroimage. 2002;15(3):686–90.

Subramony SH, May W, Lynch D, Gomez C, Fischbeck K, Hallett M, et al. Measuring Friedreich ataxia: Interrater reliability of a neurologic rating scale. Neurology. 2005;64(7):1261–2.

Taskin B, Jungehulsing GJ, Ruben J, Brunecker P, Krause T, Blankenburg F, et al. Preserved responsiveness of secondary somatosensory cortex in patients with thalamic stroke. Cereb Cortex. 2006;16(10):1431–9.

Taulu S, Simola J, Kajola M. Applications of the signal space separation method. Signal Process IEEE 2005.

Taylor MJ. Auditory brainstem responses in Friedreich's ataxia. Vol. 14, Annals of neurology. United States; 1983. p. 596–7.

Taylor MJ, McMenamin JB, Andermann E, Watters G V. Electrophysiological investigation of the auditory system in Friedreich's ataxia. Can J Neurol Sci. 1982 May;9(2):131–5.

De Tiège X, de Beeck MO, Funke M, Legros B, Parkkonen L, Goldman S, et al. Recording epileptic activity with MEG in a light-weight magnetic shield. Epilepsy Res . 2008;82(2–3):227–31.

Tinazzi M, Mauguiere F. Assessment of intraspinal and intracranial conduction by P30 and P39 tibial nerve somatosensory evoked potentials in cervical cord, brainstem, and hemispheric lesions. J Clin Neurophysiol. 1995;12(3):237–53.

Vanasse M, Garcia-Larrea L, Neuschwander P, Trouillas P, Mauguière F. Evoked Potential Studies in Friedreich's Ataxia and Progressive Early Onset Cerebellar Ataxia. Can J Neurol Sci / J Can des Sci Neurol. 1988;15(03):292–8.

Vavla M, Arrigoni F, Nordio A, De Luca A, Pizzighello S, Petacchi E, et al. Functional and Structural Brain Damage in Friedreich's Ataxia. Front Neurol. 2018;9:747.

Vigário RN. Extraction of ocular artefacts from EEG using independent component analysis. Electroencephalogr Clin Neurophysiol. 1997;103(3):395–404.

Virtanen J, Ahveninen J, Ilmoniemi RJ, Naatanen R, Pekkonen E. Replicability of MEG and EEG measures of the auditory N1/N1m-response. Electroencephalogr Clin Neurophysiol. 1998;108(3):291–8.

Wacongne C, Labyt E, van Wassenhove V, Bekinschtein T, Naccache L, Dehaene S. Evidence for a hierarchy of predictions and prediction errors in human cortex. Proc Natl Acad Sci U S A. 2011;108(51):20754–9.

Wens V, Marty B, Mary A, Bourguignon M, Op de Beeck M, Goldman S, et al. A geometric correction scheme for spatial leakage effects in MEG/EEG seed-based functional

connectivity mapping. Hum Brain Mapp. 2015;36(11):4604–21.

Wienbruch C, Candia V, Svensson J, Kleiser R, Kollias SS. A portable and low-cost fMRI compatible pneumatic system for the investigation of the somatosensensory system in clinical and research environments. Neurosci Lett. 2006;398(3):183–8.

Wikstrom H, Huttunen J, Korvenoja A, Virtanen J, Salonen O, Aronen H, et al. Effects of interstimulus interval on somatosensory evoked magnetic fields (SEFs): a hypothesis concerning SEF generation at the primary sensorimotor cortex. Electroencephalogr Clin Neurophysiol. 1996;100(6):479–87.

Yamashiro K, Inui K, Otsuru N, Kida T, Akatsuka K, Kakigi R. Somatosensory off-response in humans: an ERP study. Exp Brain Res. 2008;190(2):207–13.

Yamashiro K, Inui K, Otsuru N, Kida T, Kakigi R. Somatosensory off-response in humans: an MEG study. Neuroimage. 2009;44(4):1363–8.

Zalesky A, Akhlaghi H, Corben LA, Bradshaw JL, Delatycki MB, Storey E, et al. Cerebello-cerebral connectivity deficits in Friedreich ataxia. Brain Struct Funct. 2014;219(3):969–81.

Zegers de Beyl D, Delecluse F, Verbanck P, Borenstein S, Capel P, Brunko E. Somatosensory conduction in vitamin B12 deficiency. Electroencephalogr Clin Neurophysiol. 1988;69(4):313–8.

Zhang HQ, Murray GM, Turman AB, Mackie PD, Coleman GT, Rowe MJ. Parallel processing in cerebral cortex of the marmoset monkey: effect of reversible SI inactivation on tactile responses in SII. J Neurophysiol. 1996;76(6):3633–55.

Zouari M, Feki M, Ben Hamida C, Larnaout A, Turki I, Belal S, et al. Electrophysiology and nerve biopsy: comparative study in Friedreich's ataxia and Friedreich's ataxia phenotype with vitamin E deficiency. Neuromuscul Disord. 1998;8(6):416–25.

Tables and Figures

Table 1. Clinical characteristics of the 15 FRDA patients with GAA1 triplet expansion

Characteristics of FRDA participants (mean ± SD). GAA1: number of GAA1 triplet expansion on the shortest allele; SARA: score on the Scale for the Assessment and Rating of Ataxia. R= right / L= left. * Sub-Items of the SARA score rated between 0 (no deficit) to 4 (impossible to perform the task). Of note, all patients performed either similarly with both hands or better with the dominant hand, and difference between hands never exceeded 1 point. TER: tactile evoked response. cSI: contralateral primary somatosensory cortex. cSII: contralateral secondary somatosensory cortex.

Age (Years)	27.8 ± 12.6s
GAA1	706 ± 206
Age of onset (Year)	12.4 ± 6.2
Disease duration (Years)	15.4 ± 10.1
SARA score	22.3 ± 7.5
Upper-limb function Finger Chase* (R/L) Nose-Finger Test* (R/L) Fast alternating hand movements* (R/L) Nine-Hole Peg Test (seconds, R/L) Tactile discrimination present (n,%)	 1.69±0.91/1.81±0.94 1.44±1.27/1.93±1.14 2.56±0.60/2.87±0.48 85.4±42.3/112.2±64.6 15 (100%)
Tactile evoked responses TER at cSI (n, mean latency ±SD, mean amplitude ±SD) smMMN at cSII (n, mean latency ±SD, mean amplitude ±SD)	 15/15, 56±20.3 msec, 0.28 ± 0.16 dSPM Units 6/15, 134± 28.7 msec 0.37 ± 0.16 dSPM Units

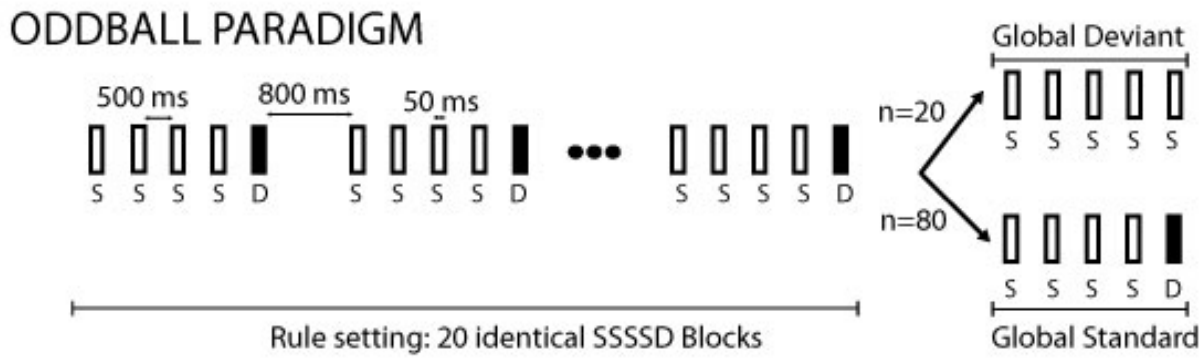

Figure 1

Sensory oddball paradigm used in this study. Blocks of five stimuli either comprised four *Standard* (S) stimuli followed by a *Deviant* (D*)* stimulus (SSSSD blocks) or 5 *Standard* stimuli (SSSSS blocks). Each *Deviant* stimulus in SSSSD blocks (local deviation) broke a sequence of four identical stimuli, thereby eliciting a MMN response.

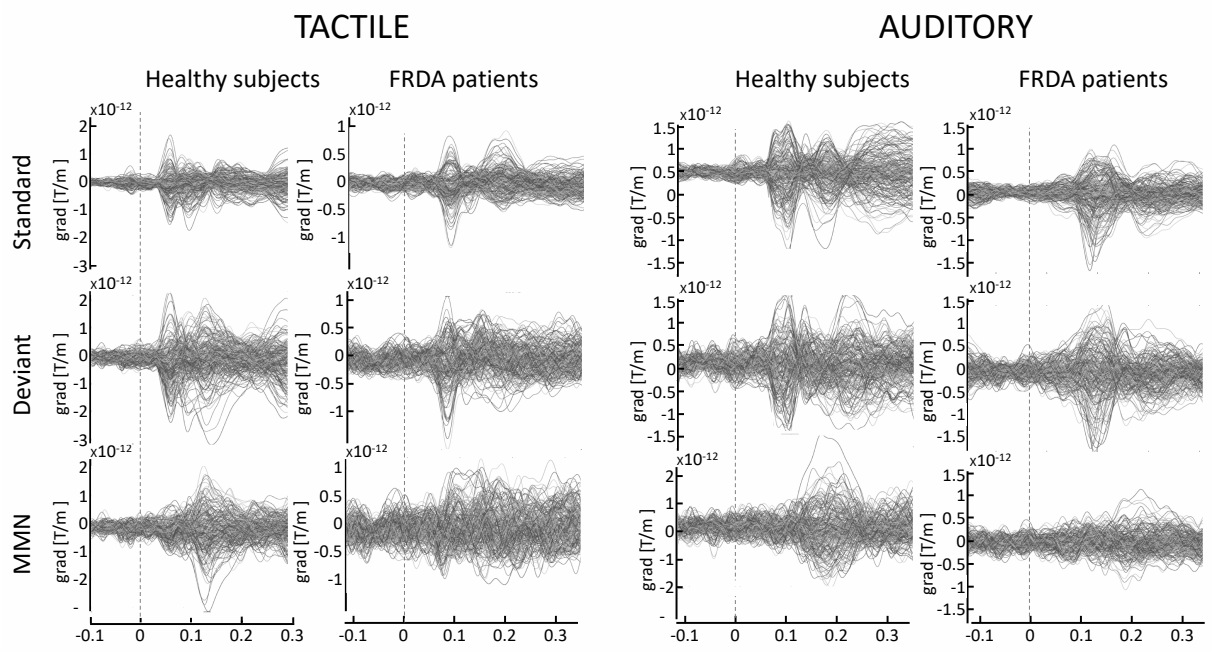

Figure 2

Butterfly plots (planar gradiometers) of the grand averaged sensor-level responses elicited by standards (upper line) and deviants (middle line) as well as of the mismatch negativity (MMN, bottom line) response for each modality and group. Each line in the butterfly plots represents the signal of one of the 204 planar gradiometers.

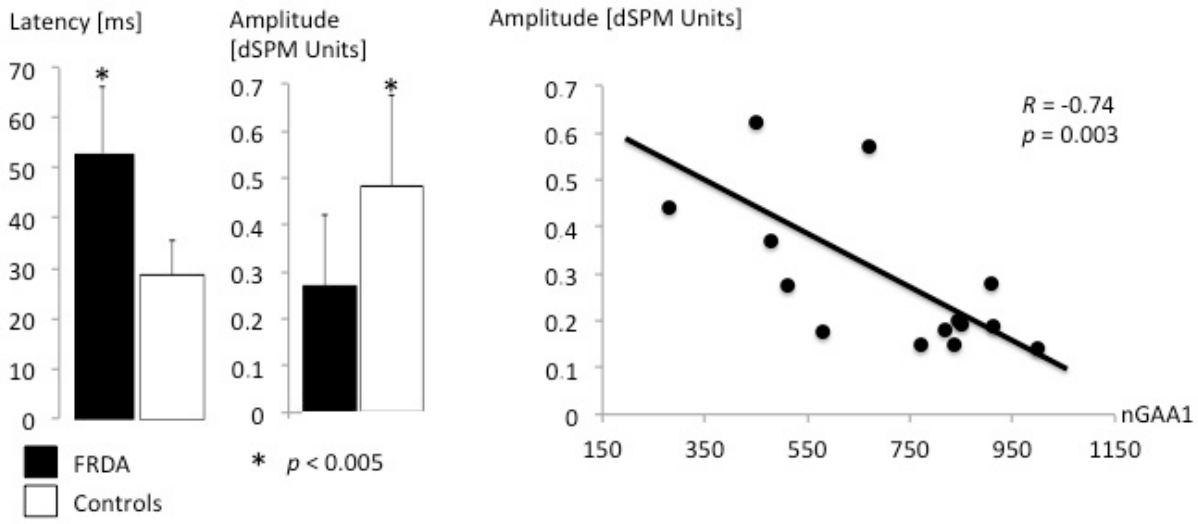

Figure 3

Somatosensory evoked responses elicited by standards. **Left**. Averaged amplitude and latency in FRDA patients (black histogram) and healthy subjects (white histogram) of the first peak of somatosensory response at left primary cSI cortex. * = statistical difference with $p < 0.001$. **Right**. Spearman correlation plot between FRDA patients' individual amplitude of cSI cortex response and the number of GAA1 triplet expansion on the shortest allele (nGAA1).

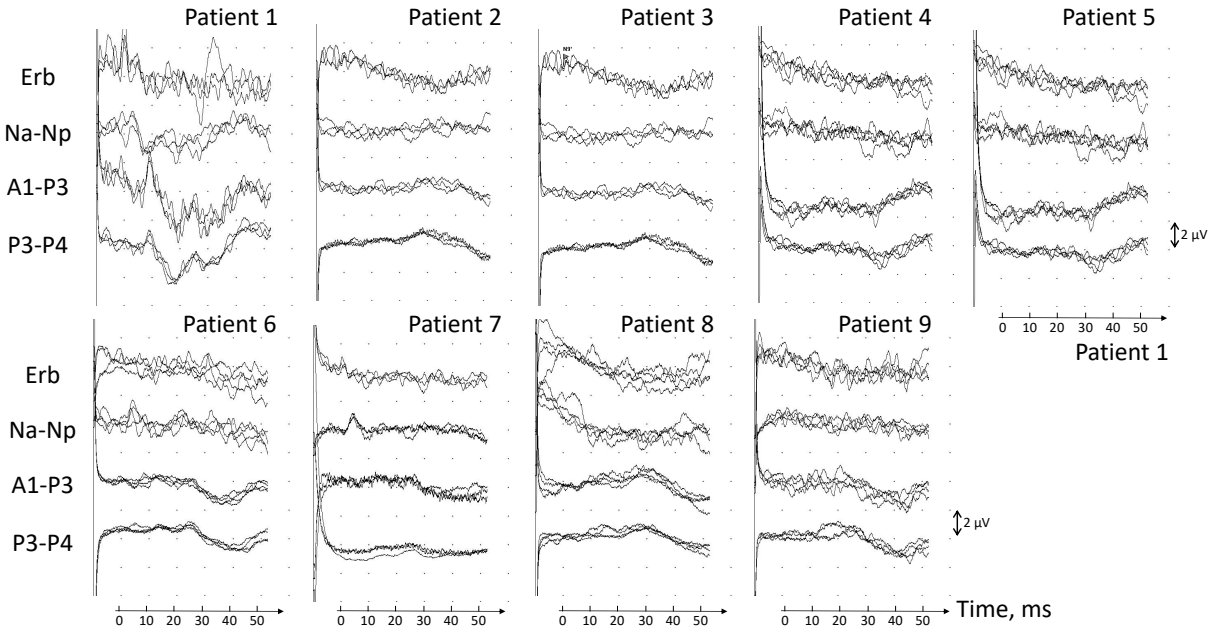

Figure 4

SSEPS raw recordings in each of nine FRDA patients who underwent the investigation. Each line corresponds to an electrode. Erb stands for Erb's point electrode, Na and Np for neck anterior and posterior electrodes, P3 and P4 for left and right parietal electrodes and A1 for left ear electrode.

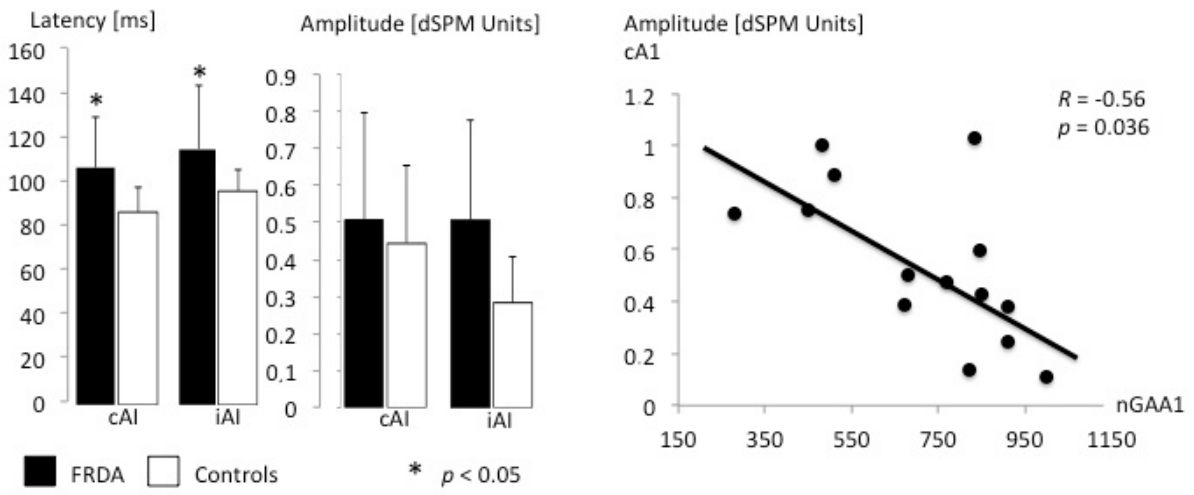

Figure 5

Auditory evoked responses elicited by standards. **Top,Left**. Averaged latency in FRDA patients (black histogram) and healthy subjects (white histogram) of the first peak of auditory response at left (cAI) and right (iAI) AI cortices. * = statistical difference with $p < 0.001$. **Right**. Spearman correlation plot between FRDA patients' individual latency at cAI cortex. **Bottom,Left**. Averaged amplitude of the first peak of auditory response at cAI and iAI cortices. **Right**. Spearman correlation plot between FRDA patients' individual amplitude at cAI cortex and the number of GAA1 triplet expansion on the shortest allele (nGAA1).

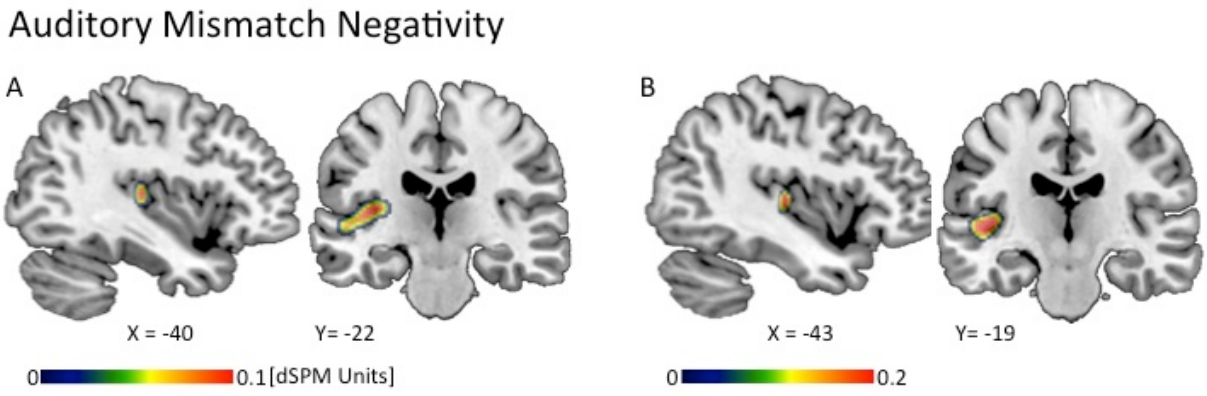

Figure 6.

Somatosensory mismatch negativity (smMMN) responses. **A.** Location and amplitude of statistically significant smMMN in healthy controls at SII cortex (MNI coordinates: [-46 -25 24] mm) at 63–139 ms post deviant stimuli. **B.** Location and amplitude of statistically significant smMMN in FRDA patients above cSII cortex ([-49 -19 19] mm) at 114–170 ms post deviant stimuli. **C**. Location and amplitude of statistically significant difference in smMMN responses between healthy subjects and FRDA patients at cSII cortex after smMMN group level maximum peak temporal realignment (MNI coordinates: [-40 -25 30] mm). **D**. Spearman correlation plot between FRDA patients' individual smMMN amplitude at cSII cortex and the number of GAA1 triplet expansion on the shortest allele (nGAA1).

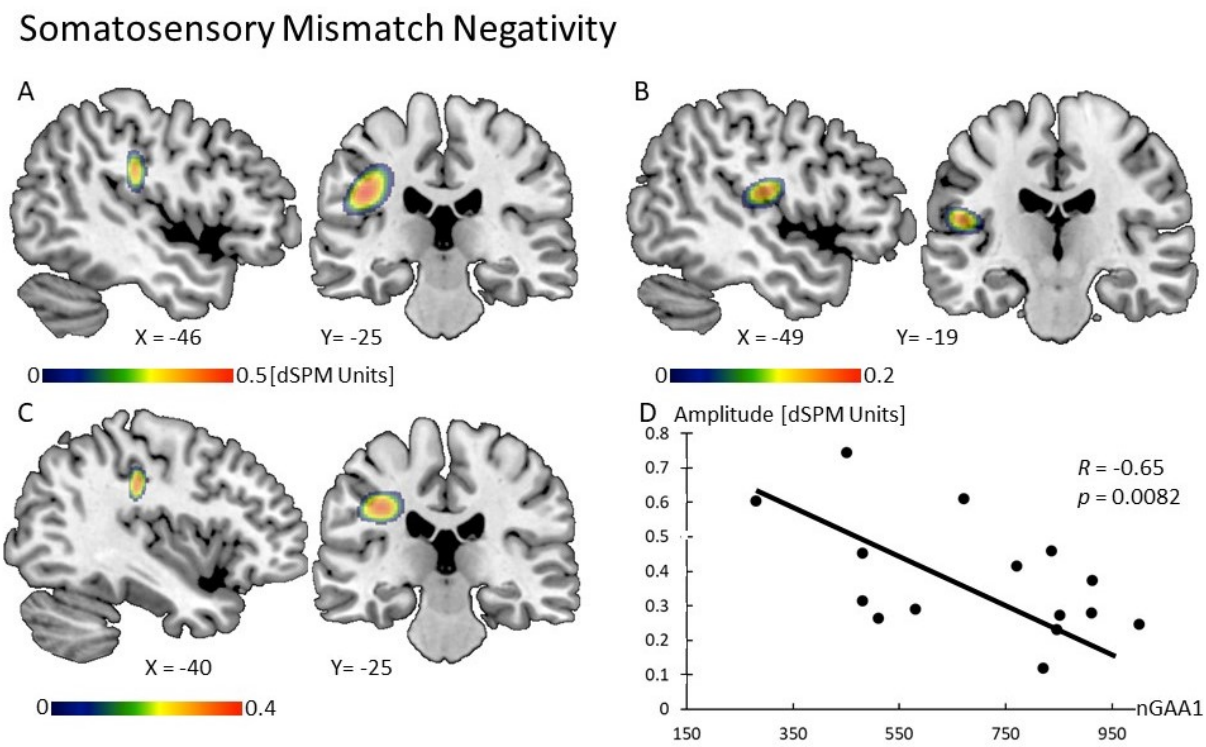

Figure 7.

Auditory mismatch negativity (amMMN) responses. **A.** Location and amplitude of statistically significant amMMN responses in healthy subjects above left AI cortex (MNI coordinates: [-40 -22 9] mm) at 162–172ms post deviant stimulus. **B.** Location and amplitude of statistically significant amMMN in FRDA patients above left AI cortex (MNI coordinates: [-43 -19 6] mm) at 150–180 ms post-deviant stimulus.